Continuous Switching of Ultra-High Voltage Silicon Carbide MOSFETs

Argenis V. Bilbao, James A. Schrock, Mitchell D. Kelley, Emilly Hirsch, William B. Ray, Stephen B. Bayne and Michael G. Giesselmann

Department of Electrical & Computer Engineering
Texas Tech University
Lubbock, USA

***Abstract*— Silicon carbide power semiconductor devices are capable of increasing the power density of power electronics systems [1, 2]. In recent years, devices rated to block voltages up to 20 kV have been demonstrated [3]. These research grade devices must be fully characterized to determine operating characteristics as well as failure mechanisms. The purpose of this paper is to demonstrate the continuous switching performance of ultra-high voltage metal oxide semiconductor field effect transistors (MOSFET) rated for 15 kV / 10 A. A high voltage boost converter was developed to evaluate the continuous switching performance where the high-voltage MOSFET is utilized as the main switching element. During operation, the on-state voltage, gate leakage current, and dc characteristics are monitored to determine device degradation. Measured device degradation is presented as a comparison of initial and final dc characterization.**

Keywords—silicon carbide; SiC; 15 kV; MOSFET; degradation; switching; boost converter

I. INTRODUCTION

Silicon has been the semiconductor material of choice for power semiconductor devices for many decades [4]. The defect density of silicon wafers is presently very low. This allow engineers to fabricate very robust and reliable power semiconductor devices. Currently, the performance of silicon-based power semiconductor devices is reaching the theoretical limit. For this reason, scientists are exploring new semiconductor materials in order to create new devices with far enhanced capabilities. Practical silicon-based metal oxide semiconductor field effect transistors (MOSFET), are limited to block voltages less than 1,200 V. This limitation occurs as a result of the prohibitively wide epitaxial layer required to create a higher voltage device with low on-state resistance. Being a majority carrier device, MOSFETs can't take advantage of conductivity modulation as the insulated gate bipolar transistors (IGBT) do. Additionally, at room temperature the intrinsic carrier concentration of silicon is $1.4x10^{10}$ cm^{-3} [5]. At 150˚C the intrinsic carrier concentration increases to $1x10^{14}$ cm^{-3} [5] which severely hinders the device's efficiency.

Silicon carbide (SiC) is a suitable upgrade for high voltage power semiconductor devices. In addition to its inherently lower intrinsic carrier concentration, the critical electric field of SiC is substantially higher than that of silicon. At room temperature the intrinsic carrier concentration of SiC is $6.7x10^{-11}$ and $1.3x10^{0}$ cm^{-3} at 150˚C [5]. Along with material characteristics like this, the higher thermal conductivity of SiC make it a very attractive alternative to silicon-based devices. Silicon carbide-based MOSFETs have been previously shown in scientific literature with blocking voltages as high as 15 kV [6, 7]. This paper describes a system developed to evaluate the continuous switching reliability of ultra-high voltage SiC power semiconductor devices. The results obtained from continuously switching a sample device will be shown and analyzed.

II. RESISTIVE AND INDUCTIVE SWITCHING TESTBED

Before performing the continuous switching tests on the 15 kV MOSFET devices, single pulse resistive switching and double pulse inductive switching tests were performed on the MOSFET. The purpose of these tests was to extract fundamental switching parameters like rise time, fall time, turn-on delay, turn-off delay, turn-on energy, and turn-off energy. Additionally, these tests proved that the devices were robust enough to handle the stress of continuous switching. Other semiconductor switches like IGBTs, bipolar junction transistors (BJT), and thryristors can also be characterized in this testbed. A single die of 15 kV MOSFETs have a continuous current rating of 10 A. This means that the maximum power that each device can switch is 150 kW. A power supply that can deliver 150 kW is prohibitively large and expensive. For this reason, this testbed utilizes a bank of capacitors to source the required current at the test voltage for a predetermined amount of time. Fig 1 shows a simplified schematic diagram of the resistive and inductive switching testbed.

A rapid capacitor charger [8, 9] is used to charge the capacitor bank formed by C1, C2, and C3 to the required test voltage. If resistive switching tests are being performed, L and D are replaced with shorts. In this case, the current flows from the capacitor bank through RL, the device under test (DUT), and finally to ground. The test current is dictated by the resistor value and the capacitor bank voltage. In the case of

inductive switching tests all the components shown in Fig 1 are used. The resistor labeled RL is kept in the system for safety purposes. If the device were to fail to short, RL would limit the maximum current flowing through the device. Limiting the current helps prevent explosions as a result of excessive current flow. The diode shown in the schematic diagram creates a freewheeling path for the current when the device is switching from the on-state to the off-state. The gate driver shown in the schematic diagram is the IXDI604PI from IXYS Integrated Circuits. This gate driver is capable of supplying up to 4 A to the gate of the DUT for fast switching if needed. A function generator is used to generate a pulse of the required width to conduct the tests. The signal produced by the function generator is converted to an optical signal and transmitted to the testbed using a plastic fiber optic cable. This practice gives an additional layer of safety against high voltage.

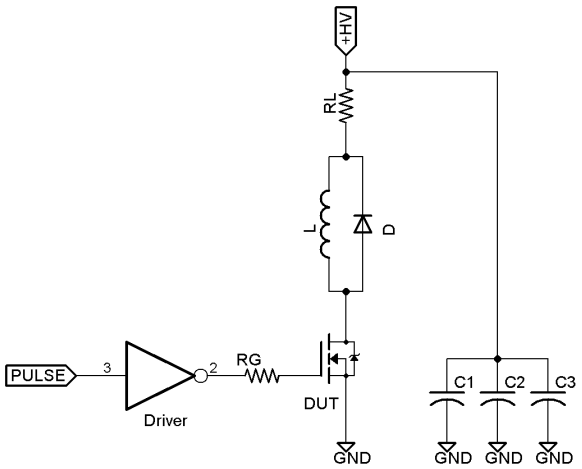

Fig 1. Simplified resistive and inductive switching testbed schematics.

III. Results of The Resistive and Inductive Switching Tests

The resistive and the inductive switching tests were performed from room temperature to 150˚C in steps of 25˚C. The resistive switching tests were used to extract current rise times, current fall times, turn-on delays, and turn-off delays as a function of case temperature. Table I shows the test parameters used for the resistive switching tests. Initially the device's forward conduction curves and breakdown IV curves were extracted. These initial IV curves were used as a baseline in order to monitor degradation as a result of switching stress.

TABLE I. Resistive switching test parameters.

Gate Turn-on Bias	25 V
Gate Turn-off Bias	-5 V
Gate Resistor	27 Ω
Drain-to-Source Voltage	11 kV
Load Resistor	1.1 kΩ
Pulse Width	52 µs

The results of the resistive switching tests are shown in Table II. As it can be seen in this table, the current rise time and the turn-on delay have a descending trend while the current fall time and the turn-off delay has an ascending trend. This occurs as a result of the change in plateau voltage as a function of temperature. All the parameters extracted from the resistive switching tests are a strong function of the plateau voltage which in turn is a function of the gate threshold voltage. As the gate voltage drops as a function of increased temperature, it takes less time for the gate voltage to reach the plateau voltage at which point the drain current start to increase. For this reason, the rise and the turn-on delay become less as temperature increases. Similarly, when the gate voltage is at the turn-on bias, it takes longer time to reach the plateau voltage before the current starts to fall. This causes longer fall times and turn-off delays as temperature increases.

TABLE II. Resistive switching test results.

Case Temp.	Rise Time	Fall Time	Turn-on Delay	Turn-off Delay
25˚C	177 ns	280 ns	152 ns	245 ns
50˚C	158 ns	283 ns	145 ns	257 ns
75˚C	146 ns	288 ns	139 ns	267 ns
100˚C	137 ns	295 ns	136 ns	276 ns
125˚C	132 ns	302 ns	132 ns	285 ns
150˚C	127 ns	307 ns	129 ns	293 ns

The inductive switching tests were performed with the parameters shown in Table III. The turn-on/off gate bias, the gate resistor, and the drain to source current remained the same but the load resistor was lowered to 200 Ω, the load inductor was set to 16 mH, and a 15 kV SiC P-*i*-N diode was added. Instead of performing a single pulse, two pulses are required in order to obtain the same current at turn-on and turn-off.

TABLE III. Resistive switching test parameters.

Gate Turn-on Bias	25 V
Gate Turn-off Bias	-5 V
Gate Resistor	27 Ω
Drain-to-Source Voltage	11 kV
Load Resistor	200 Ω
Pulse Width	18 µs
Load Inductance	16 mH
Diode Type	15 kV SiC P-*i*-N

The MOSFET's turn-on and turn-off energy show minuscule changes as a function of temperature. This is because the inductive switching energies are mostly dictated by the system itself and not so much about the device being switched. One interesting fact is that the turn-on energy is significantly higher than the turn-off energy. This is because at turn-on the freewheeling diode's reverse recovery current. With a momentarily high current spike, the turn-on energy is greatly incremented. The amount of reverse recovery current

is dependent on the diode used. In this particular case the turn-on energy is 5.2 times higher than the turn-off energy.

After performing all the inductive and resistive switching tests the initial curves and the curves after performing the tests were compared. Fig 2 shows the comparison between the initial breakdown IV curve and the IV curve extracted after the tests. As it can be seen in this curve, no degradation occurred after single and double pulse testing. These tests provided important transient characteristics of the DUT and provided proof that the devices were robust enough to be subjected to more stringent testing like the continuous switching tests.

TABLE IV. INDUCTIVE SWITCHING TEST RESULTS.

Cate Temperature	Turn-on Energy	Turn-off Energy
25˚C	33.85 mJ	6.53 mJ
50˚C	32.48 mJ	6.54 mJ
75˚C	32.20 mJ	6.57 mJ
100˚C	32.29 mJ	6.54 mJ
125˚C	32.21 mJ	6.65 mJ
150˚C	32.21 mJ	6.65 mJ

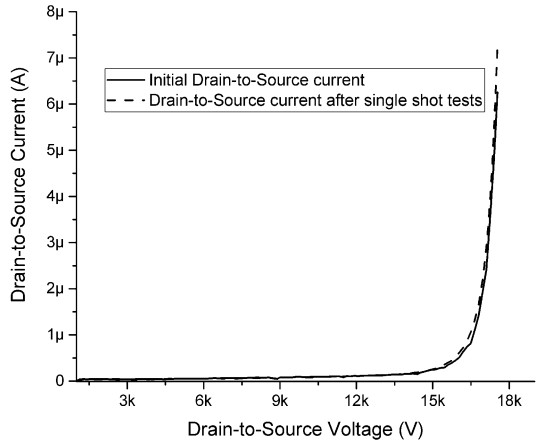

Fig 2. Comparison between the initial breakdown IV curve and the breakdown IV curve after performing the resistive and insductive switching tests.

IV. CONTINUOUS SWITCHING TESTBED

Different sub-systems come together to form the continuous switching testbed used to stress the devices beyond the limits imposed by single pulse resistive and double pulsed inductive switching tests. This testbed uses a discontinuous conduction mode boost converter as a tool to continuously switch the DUT. The DUT is used as the main switching element of the boost converter. The converter is fed by a custom-built high voltage power supply. This power supply takes an input ac current from a three-phase variable transformer and further steps-up the voltage as required by the test being performed. The output of the boost converter is dissipated in a high-power, high-voltage power resistor bank. Fig 3 shows a block diagram of the system.

In order to avoid potential catastrophic device failure, four safety mechanisms are featured by the continuous switching testbed. The first safety mechanism is that it is able to monitor the DUT's on-state voltage [10]. If the on-state voltage crosses over a user-specified limit, the boost converter shuts itself down and issues a signal to shut down the power supply. The second mechanism is by monitoring the DUT's gate leakage current. If the leakage current exceeds a user-defined limit the system shutdown procedure is initiated. The third safety mechanism is through the monitoring of the output voltage. If the boost converter is unloaded as a result of load bank failure the system is automatically shut down. The fourth and last safety mechanism is a manual shut down remote control that allows the user to abort the testing at will if any abnormality is detected.

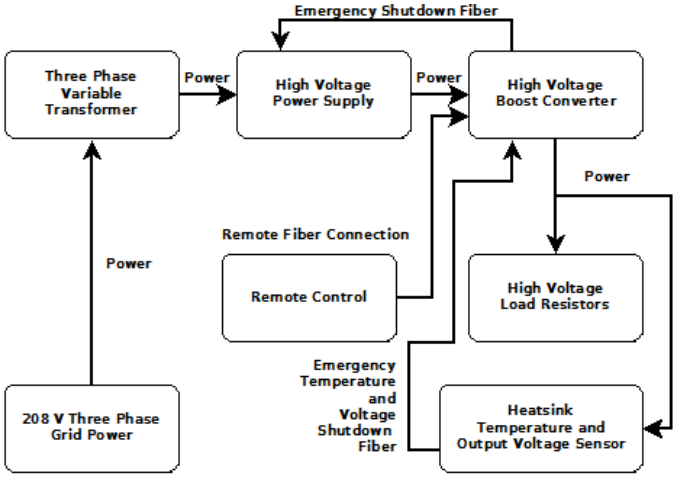

Fig 3. Continuous switching testbed simplified block diagram.

V. CONTINUOUS SWITCHING TEST RESULTS

The continuous switching tests were performed with the parameters shown in Table V. Even though no damage to the device's oxide occurred as a result of switching with a gate turn-on bias of 25 V, the gate voltage was lowered to 20 V. This decision was taken because no significant advantages were encountered by switching the device at the higher voltage. A lower turn-on bias voltage would also lessen oxide layer stress.

TABLE V. CONTINUOUS SWITCHING TEST PARAMETERS.

Gate Turn-on Bias	20 V
Gate Turn-off Bias	-5 V
Gate Resistor	4.99 Ω
Input Voltage	1080 V
Output Voltage	10 kV
Switching Frequency	1 kHz
Duty Cycle	22.5 %
Peak Device Current	11.4 A
Continuous Output Power	1031 W

In order to gain confidence in the DUT and the system, the tests were performed in short durations sessions. As the sessions terminated, the subsequent sessions had longer durations. At the end of each session, the device was characterized in forward conduction mode and in blocking mode to monitor degradation. Table VI shows the session information for the 15 kV MOSFET.

TABLE VI. SESSION NUMBERS AND DURATIONS FOR THE 15 KV MOSFET.

Session Number	Session Duration	Total Switching Time
1	5 minutes	5 minutes
2	10 minutes	15 minutes
3	20 minutes	35 minutes
4	30 minutes	65 minutes
5	60 minutes	125 minutes

This device switched for a total of 125 minutes with an output voltage of 10 kV and a peak current of 11.4 A. At no moment in time the testbed stopped the tests as a result of parameters crossing the user-specified threshold voltage or any of the other parameters. Fig 4 shows a comparison between the initial breakdown IV curve and the IV curves taken at the end of each one of the switching sessions. As it can be seen in this figure, no degradation occurred in the blocking voltage capability of the device. Similarly, no degradation occurred in the forward conduction capability of the device under test.

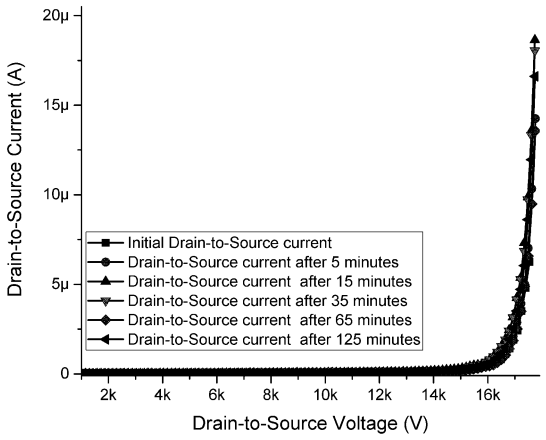

Fig 4. 15 kV MOSFET breakdown characteristic comparison.

VI. CONCLUSION

In this paper a sample 15 kV MOSFET was used to perform resistive and inductive switching tests in order to extract the current rise times, current fall times, turn-on delays, turn-off delays, turn-on energies, and turn-off energies. These were performed in a testbed specifically developed for this purpose. The results from the resistive and inductive switching tests proved that the devices were robust enough to be subjected to more stringent tests. Similarly, a testbed was developed to subject the 15 kV MOSFET to continuous switching tests. The testbed was discussed and the test parameters were shown. Results of the continuous switching tests were presented by comparing the breakdown IV curves before and after the tests were performed. No degradation was encountered on the device after the tests were performed.

ACKNOWLEDGMENT

This research was sponsored by the Army Research Laboratory under a subcontract from Wolfspeed – a Cree Company and was accomplished under Cooperative Agreement Number W911NF-10-2-0038. The views and conclusions contained in this document are those of the authors and should not be interpreted as representing the official policies, either expressed or implied, of the Army Research Laboratory, the U.S. Government or Cree, Inc. The U.S. Government is authorized to reproduce and distribute reprints for Government purposes notwithstanding any copyright notation hereon.

REFERENCES

[1] J. A. Schrock *et al*., "High-Mobility Stable 1200-V, 150-A 4H-SiC DMOSFET Long-Term Reliability Analysis Under High Current Density Transient Conditions," *IEEE Trans. Power Electron.*, vol. 30, no. 6, pp. 2891-2895, Jun. 2015.

[2] L. Cheng *et al*., "20 kV, 2 cm^2 4H-SiC gate turn-off thyristors for advanced pulsed power applications," in *2013 19th IEEE Pulsed Power Conference (PPC)*, San Francisco, CA, 2013, pp. 1-4.

[3] A. V. Bilbao, J. A. Schrock, W. B. Ray, M. D. Kelley and S. B. Bayne, "Analysis of advanced 20 KV/20 a silicon carbide power insulated gate bipolar transistor in resistive and inductive switching tests," in *2015 IEEE Pulsed Power Conference (PPC)*, Austin, TX, 2015, pp. 1-3.

[4] G. Ouimet, D. L. Rath, S. L. Cohen, E. E. Fisch and G. W. Gale, "Defect reduction and cost savings through re-inventing RCA cleans," in *IEEE/SEMI 1996 Advanced Semiconductor Manufacturing Conference and Workshop. Theme-Innovative Approaches to Growth in the Semiconductor Industry. ASMC 96 Proceedings*, Cambridge, MA, 1996, pp. 308-313.

[5] B. J. Baliga, "Material Properties and Transport Physics," in *Fundamentals of Power Semiconductor Devices*, New York, NY, USA:Springer-Verlag, 2008.

[6] V. Pala *et al*., "10 kV and 15 kV silicon carbide power MOSFETs for next-generation energy conversion and transmission systems," in *2014 IEEE Energy Conversion Congress and Exposition (ECCE)*, Pittsburgh, PA, 2014, pp. 449-454.

[7] J. W. Palmour *et al*., "Silicon carbide power MOSFETs: Breakthrough performance from 900 V up to 15 kV," in *2014 IEEE 26th International Symposium on Power Semiconductor Devices & IC's (ISPSD)*, Waikoloa, HI, 2014, pp. 79-82.

[8] M. G. Giesselmann and A. Bilbao, "Digital control of a rapid capacitor charger with sensor-less voltage feedback," *IEEE Trans. Dielectr. Electr. Insul.*, vol. 22, no. 4, pp. 1930-1936, Aug. 2015.

[9] M. G. Giesselmann and A. Bilbao, "Digital control of a rapid capacitor charger with sensor-less voltage feedback," in *2014 IEEE International Power Modulator and High Voltage Conference (IPMHVC)*, Santa Fe, NM, 2014, pp. 640-643.

[10] A. V. Bilbao *et al.*, "Development and testing of an active high voltage saturation probe for characterization of ultra-high voltage silicon carbide semiconductor devices," *Rev. Sci. Instrum.*, vol. 86, pp. 85-104, Aug. 2015.